Aerial 5G Non-Public Networks: Link Budget, Coverage, and Capacity Analysis

Jyrki T. J. Penttinen
Alphacore Inc.
Tempe, AZ, USA
jyrki.penttinen@alphacoreinc.com

Garth V. Rees
VERN Consulting
Madrid, Spain
garth.rees@verncon.net

Urs C. Schlegel
Independent Researcher
Munich, Germany
urs.c.schlegel@mail.com

***Abstract*—Uncrewed Aerial Vehicles (UAVs) equipped with radios can establish rapid, ad-hoc connectivity in areas where terrestrial infrastructure is unavailable or compromised. Leveraging the virtualized architecture of Fifth Generation (5G) mobile networks, both base station and required minimal core functions can be hosted aloft, enabling agile Internet of Things (IoT) or evolved Mobile Broadband (eMBB) centric private networks for emergency response, expeditionary, military operations, and consumer events. This study evaluates the technical feasibility of UAV-mounted 5G Non-Public Network assembled from commercial off-the-shelf components, comparing the physical radio layer performance of IoT and evolved mobile broadband use cases. Candidate 3GPP architectural options are reviewed, and radio link budget calculations quantify physical layer performance in open and rural environments for a single-UAV. Simulations in dense area type complement the study presenting the impact of UAV height in a single UAV case and a formation of three UAVs. The obtained results highlight the trade-off between frequency band, UAV-altitude, and the resulting radio coverage and data rate, providing design guidance for lightweight, energy-efficient aerial 5G systems.**

Keywords-aerial 5G network; link-budget analysis; uncrewed aerial vehicle (UAV); non-public network (NPN); drone-mounted IoT and eMBB radio service; emergency communications; ad-hoc radio access network (RAN); radio coverage and capacity estimate.

I. Introduction

Apart from their commercial use, cellular systems can be deployed also as complementing ad-hoc networks, e.g., in emergency solutions after a natural disaster that has damaged telecommunications infrastructure, or in scenarios where non-permanent augmented capacity and radio coverage are desired. A Fifth Generation (5G) private mobile network model through temporally deployed base stations can provide a suitable platform for data transfer and signaling in such situations, enabling enhanced communications and situation awareness also for, e.g., defense groups.

However, in temporal ad-hoc use cases, 5G users may be highly mobile, so deploying terrestrial trailer-mounted radio base stations may not suffice, as the varying link conditions alter quality and can result in uncertainties, resulting in radio network outages when users are on the move. An aerial ad-hoc 5G network that follows the underlying users can provide an important opportunity to overcome these challenges.

Based on the originally published study "Design Feasibility and Link Budget Assessment of Aerial 5G IoT and eMBB Connectivity" [1], this paper presents an extended feasibility study of a UAV-based 5G radio network that can be used in various Line of Sight (LOS) scenarios through 5G Non-Public Networks (NPNs).

The 3rd Generation Partnership Project (3GPP) is developing the Internet of Things (IoT) concept further in 5G as a logical continuum from the 4G era, in terms of massive Machine Type Communications (mMTC). 5G IoT in 3GPP is realized through legacy Long-Term Evolution (LTE) -based Narrow-Band IoT (NB-IoT) and LTE for Machines (LTE-M) seamlessly attached to the 5G Core Network (CN) and, from Release 17 onward, through 5G New Radio (NR) Reduced Capabilities (RedCap), which is a native, reduced-bandwidth flavor of NR, and evolves further as of Release 18 [2]. Combining NPN and IoT through aerial platform enables novel means to develop and provide low-power, low-data rate services in very large areas.

The novelty of this research lies in the following: 1) it presents a concept based on 3GPP-defined NPN-architecture and available Commercial Off-the-Shelf (COTS) components to provide aerial IoT and data services to a variety of use cases and 2) it evaluates performance of such a solution comparing UAV-mounted 5G next generation Node B (gNB) performance of evolved Mobile Broadband (eMBB) and mMTC.

This study considers UAVs for local communication to a set of User Equipment (UE) underneath, paving the way for the forthcoming work that will consider the formation of a multi-UAV-based 5G RAN service and automatized location functions through advanced sensing and artificial intelligence.

Section II discusses the state-of-the art of UAV-assisted wireless communication and current gaps. Section III presents IoT and eMBB, and Section IV discusses 3GPP-defined 5G NPN. Section V describes a 5G-UAV concept and discusses UAV-mounted equipment, presenting an example of a feasible set. Section VI describes physical radio aspects, and Section VII presents link budget results for validation of radio network performance applying adequate radio propagation modeling for aerial network and comparing 5G eMBB and IoT use cases that represent two “extremes” in terms of achievable 3D-network coverage areas. Based on in-house -developed software, Section VIII presents radio network coverage and achievable data rate simulations in a combined dense urban and open environment of Sydney, Australia, considering the impact of UAV altitude for a single UAV-housed gNB and a set of gNBs in three UAV constellation. Section IX summarizes the observations of this study and Section X presents our plan for further research.

II. UAV-Assisted Networking

The global 5G deployments are expanding. The GSM Association (GSMA) estimates that the adaption for 5G will surpass that of 4G in 2028, whereas the earlier networks, 2G and 3G, keep losing their customers; in fact, many of these networks have already been decommissioned [3].

Figure 1 presents an assessment of the data available from [3], showing that soon after 5G has become the dominating mobile communications technology, it also surpasses the sum of the users of all the previous generations 2G, 3G, and 4G.

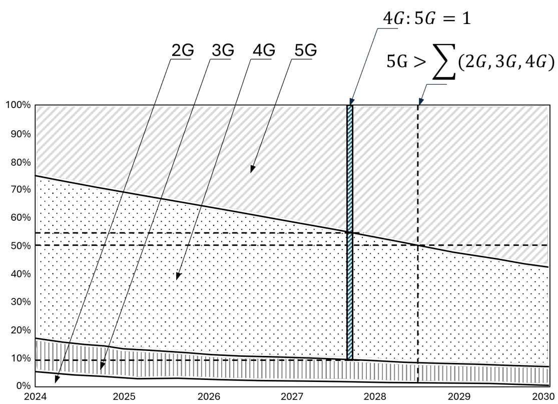

Figure 1. Mobile adoption by technology: percentage of total connections

The current 5G system architecture models enable various deployment options and variations for tailored solutions. Examples of these facilitators include new NPN architectures, Non-Terrestrial Networks (NTNs), Open RAN, and mMTC that are all evolving and being deployed in commercial networks.

While 5G matures, there are already concrete efforts to develop systems beyond 5G (B5G), paving the way for Sixth Generation (6G) [4]. During Release 20, 3GPP has carried out use case and feasibility studies, and the actual forming of technical 6G specifications begins along with the Release 21. The first commercial 6G networks can be expected to be available as of 2030 [5]. The 6G is anticipated to be particularly attractive for connected UAVs due to significant improvements, including ubiquitous 3D connectivity on the ground and in the air [6].

While 6G is still under development, the current 5G systems outperform the previous generations, and can be tailored to provide radio service also beyond traditional terrestrial base stations through Service-Based Architecture (SBA) and Service-Based Interfaces (SBIs) that handle specific needs of varying use cases and dynamically provide optimal sets of required and available resources to different usage types through Network Functions Virtualization (NFV).

The key benefit of 5G is its ability to run Network Functions (NFs) on COTS hardware. This evolution makes 5G a suitable candidate also for UAV-type networking, e.g., through NPN models as they can form an architectural base for isolation (with augmented security) or interconnection / roaming (providing wider connectivity) network segment. A Mobile Network Operator (MNO) or Network Slice (NS) Provider (NSP) can set up NSs, that can be used for deploying UAV-networks, too.

5G systems can be optimized further through Open RAN (Radio Access Network). Examples of the efforts driving Open RAN include Open RAN Alliance's O-RAN [7] and Telecom Infra Project's TIP [8]. Via Open RAN, vendor-specific internal RAN interfaces are opened so that an extended number of stakeholders can provide select RAN protocol layers independently, increasing efficiency and reducing costs [9], and it can be used also in UAV-based networking [10].

As for the State of the Art and challenges, the mobile networks' radio coverage extension mounting a base station or repeater on aerial vehicle has been studied from several points of view, such as how to maximize the radio coverage by optimal UAV positioning [11] and how to enable group handover for drone base stations [12] related to the mMTC, use of data services, and commercial needs for respective coverage and capacity extension to facilitate adequate data rates and Quality of Service (QoS) for the subscribers.

On radio link budget, there are various studies such as [13] (high-altitude platform for 5G access node) and [14] (system model for forward link transmissions in an Integrated Access and Backhaul (IAB) multi-tier drone cellular network). An example of real-world UAV-based networking is AT&T's 5G Cell on Wings (CoW), a drone-mounted cellular 4G or 5G base station that temporarily extends radio coverage, e.g., during disasters and large events [15].

Nevertheless, the available studies are not necessarily conclusive in terms of the tradeoffs of the UAV altitude and wider set of deployed frequency bands [16]. Furthermore, the adaptation of optimal architectural models of UAV-networking, considering the feasibility and gaps of COTS components, can benefit from additional research [17].

III. IoT vs. eMBB

The 5G eMBB and IoT (mMTC) represent opposites in terms of many aspects, like data rates, power consumption and number of simultaneously communicating devices. These elements dictate also the achievable radio coverage area size. For example, IoT has been optimized for bandwidth given that IoT payloads are small, and narrow band lowers the thermal noise floor. IoT relies on robust modulation schemes and Hybrid Automatic Repeat Request (HARQ) repeats balancing respective throughput and coverage. It is important to note that battery-driven IoT modules stay below 1 W to meet license and life constraints (e.g., NB-IoT Class 3 and Class 5 use 23 dBm and 20 dBm, respectively). Table I summarizes some of the key differences of IoT and eMBB.

IV. Aerial Private Network Considerations

3GPP has designed private network realizations through Standalone Non-Public Network (SNPN) and Public Network Integrated Non-Public Network (PNI-NPN) models [18] as presented in Table II. Although 3GPP designed these models

TABLE I. COMPARISON OF KEY ASPECTS OF 5G EMBB AND IOT

Item	eMBB	IoT
Channel bandwidth	20 – 400 MHz	180 kHz – 20 MHz
SNR (BLER<10%)	8 – 15 dB (64 / 256 QAM)	-13 – -3 dB (BPSK / QPSK, heavy coding)
Fade/penetr. marg.	3 – 5 dB	10 – 15 dB
Device TX power	23 dBm (smartphone)	14 – 23 dBm (sensor)
Data rate target	10 Mb/s – 1 Gb/s	50 b/s – 1 Mb/s

TABLE II. PRIVATE NETWORK TYPES IN UAV-BASED DEPLOYMENTS

Variant	Assessment
SNPN (fully standalone architecture)	Best for autonomous, localized, quick-to-deploy networks (no MNO dependency)
PNI-NPN with radio access network sharing	Enables UAVs to share ground RAN where available, while maintaining separate core
PNI-NPN with core network sharing	UAV-based NPN reuses public 5G core network, allowing leaner deployment
UE route selection via mobile network selection	UEs served by UAVs can select between private and public network profiles

for terrestrial networking, their principles can be extended to serve also in aerial networks.

For the architectural modeling of 5G-based UAV network, the following technical specifications form the base: 1) 3GPP TS 23.501 (System Architecture for the 5G System) defines high-level architecture for both SNPNs and PNI-NPNs [19]; 2) 3GPP TS 23.548 (5G System Enhancements for NPN) explores enhancements specific to NPNs (e.g., management, registration, selection) [20]; and 3) 3GPP TS 22.261 (Service Requirements for 5G System) covers typical service-level requirements relevant to NPNs including verticals, e.g., public safety [21] stating also that 5G is expected to support various enhanced UAV scenarios for applications and scenarios for low altitude UAVs in commercial and government sectors.

SNPN is self-contained and independently operated from public networks. It is adequate for rapid deployment for on-demand aerial networks with no dependency on commercial MNO infrastructure and is thus a match for UAV-based temporal networks serving field units. PNI-NPN, in turn, is an NPN deployed with integration into a public mobile network, and it may share infrastructure (e.g., RAN or CN). The variants of PNI-NPN include RAN-sharing with network slicing, core network sharing, and UEs with public and private subscriptions, referring to Public Land Mobile Network (PLMN) or Network Slice Instance (NSI) selection.

Table II summarizes the 3GPP-defined NPN types and presents their key benefits related to their applicability for forming UAV-based network services.

V. 5G-CAPABLE UAV REALIZATION

The system considered in this study is based on minimal viable 5G SNPN architecture and a single UAV equipped with a 5G gNB enabling local connectivity to the UEs underneath to provide temporarily deployable service if complementing MNO infrastructure is not available.

A. Architecture

Based 3GPP SNPN models [18], Figure 2 presents a respectively adapted UAV-monted SNPN realization in this study. UAV (or set of UAVs) can house radio functions, whereas the essential core network functions of gNBs can be implemented on the same UAVs, separate UAVs, or ground station.

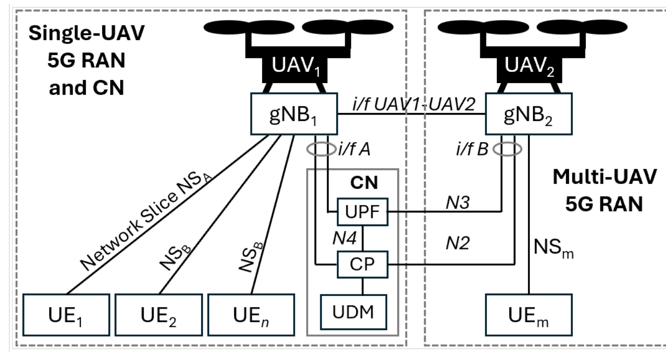

Figure 2. UAV-based, isolated SNPN realization that can be based on a single UAV or multiple interconnected UAVs that house 5G gNB

This model can be extended to cover additional UAVs and respective gNBs that are interconnected (e.g., through low-latency PC5 link between vehicles) forming a 5G RAN drone swarm, e.g., via 5G-based mesh between UAVs.

In multi-UAV 5G radio service provisioning, it can be reasoned that maintaining optimal 3D placement is hard as small altitude shifts swing path loss and backhaul Signal-to-Noise Ratio (SNR), so sufficient overlapping must be ensured. Some additional challenges include satellite positioning jitter or denial that can degrade the Time Division Duplex (TDD) timing and node loss fragments control. To overcome these challenges, control can be made hierarchical (central planner and local packet core), and use of multi-source timing can help in this. The rapid geometry changes are another challenge as they may trigger ping-pong handovers, especially in the case of narrow NR beams that raise beam-failure risk in UAV turns. Also, a dominating cell with a weak multi-hop backhaul can impact negatively the QoS. To overcome this challenge, it is possible to apply larger handover hysteresis (e.g., 3-5 dB) and time to trigger (e.g., 160-320 ms), implement dual connectivity feature (make-before-break), and use backhaul-weighted cell selection.

B. Equipment Considerations

To deploy a 5G SNPN UAV RAN, the UAV can host a basic integrated gNB (e.g., Amarisoft / Parallel Wireless). The basic location management is assumed to be manual and satellite positioning system -assisted, but automated methods can also be developed based on UE signals and using basic Radio Frequency (RF) heuristics (e.g., weighting received signal strength indicator) to position the UAVs according to user density.

Basing the solution on COTS devices, Table III presents a set of feasible candidate elements for simplified functional architecture.

TABLE III. FUNCTIONAL ARCHITECTURE OF AERIAL 5G SYSTEM

Layer	Function	Realization
Radio Access (RA)	gNB (5G standalone) with full UE-to-UE routing support	Lightweight COTS integrated into small cell
Control Plane (CP)	Lightweight distributed UAV logic (also swarm consensus)	Simple microcontroller and onboard logic
Backhaul (BH)	None (fully isolated); direct local P2P 5G	PC5 direct-mode or local user plane function (UPF)
Intel-ligence	Initially manual; advanced version has UE-following	Position, RSSI-based positioning heuristics
UE Signal-ing	Simple beaconing uplink from UEs, e.g., by Synchronization Signal Blocks (SSBs)	Existing 5G UE support
Swarm Comms	When more than one UAV, 5G-based mesh between UAVs	5G PC5 (Sidelink)

Table IV presents examples of UAV-mounted equipment. For advanced alignment of the UAVs and UEs, downward-facing cameras can be considered for UE clustering estimation (COTS-based image processing) and barometers for altitude stabilization. Based on the selected options minimizing the weight of the components, the total UAV payload (essential RAN components) is at minimum approximately 2.5–3.0 kg, which is feasible for medium-class UAVs (e.g., DJI Matrice 300 RTK [22] or similar custom UAVs).

One of the key challenges of UAV-based networking is the limitations of power supply, which represents the major weight of the payload. As an example, the above-mentioned DJI Matrice 300 RTK supports up to 55 minutes operational flight time [22]. For the communication components, Table IV presents a rough estimate of the average and peak power drain. As can be seen, the gNB consumes major part of the total power. For the operational power of the UAVs and 5G RAN components, this feasibility study assumes ideal power management, but in practice, hybrid model can be used with tethered UAVs (permanent anchor nodes with gNBs) and rotating UAVs (fly, recharge, rotate). Complementary power sources can be, e.g., solar panels (small flexible panels on UAV structure extending flight by approximately 10-20%), hydrogen fuel cells (about 2-3× endurance of lithium polymer, LiPo), or tethered power supply forming wired UAVs with unlimited power (for anchor UAVs [23]).

TABLE IV. EXAMPLES OF 5G RAN KEY EQUIPMENT PER UAV (*POWER CONSUMPTION ESTIMATED IN TYPICAL AVERAGE / PEAK WATTS)

Component	Description	Example	Weight	Power*
Integrated 5G Small Cell	Embedded gNB; RU (SA mode)	Amarisoft Callbox Mini / Baicells Nova430	400 – 800g	25 / 40W
Light Compute Module	For basic UAV / swarm logic	Raspberry Pi CM4 or Jetson Nano	100 – 200g	8 / 12W
Simple Mesh Swarm Radio	IEEE 802.11s Wi-Fi 6 / V2V PC5	Compex WLE900VX / 5G module	50 – 100g	6 / 12W
Battery Pack	Standard UAV LiPo	6S 22000 mAh	1.5 – 2.0kg	0.6 / 1W
Positioning Sensors	GPS, IMU	COTS GPS + Pixhawk FC	<100g	3 / 5W

It should be noted that regulation limits the operational boundaries in terms of UAV altitude and maximum radiated power. As an example, there is no general airborne-gNB Effective Isotropic Radiated Power (EIRP) allowance in the USA and the power is what the experimental or carrier's license and service rules permit, often with tight coordination to prevent wide-area interference. US-rules dictate 400 ft for the maximum UAV altitude above ground level (AGL) under Part 107, although higher values can be permitted via waiver. In the EU, routine airborne gNBs are not covered by the standard local/private-5G licenses, so specific or certified flight approval is needed with European Union Aviation Safety Agency (EASA) framework as well as a trial or temporary spectrum license from the national regulator, and the maximum altitude is 120 m AGL.

VI. PHYSICAL RADIO INTERFACE

This feasibility study considers theoretical coverage limits of a single UAV applying relevant propagation loss models, with the aim to provide optimal 5G RAN quality and performance as a function of UAV altitude (and later, inter-UAV distance) in rural and open areas, and the following parameters: 1) Frequency band f = low (1 GHz), mid (3.5 and 6 GHz) and high (24 and 28 GHz); 2) UAV altitude h_{gNB} = 50m, 100m,..., 400m; 3) UE type = pedestrian; 4) Power P_{UE} = +23 dBm, P_{gNB} = +23 dBm; 5) UAV antenna type is omni-directional (0 dBi gain, uniform, ideal radiation pattern). The key results include achievable cell size and respective data rate estimate for both eMBB and IoT use cases.

The starting point of the study was to consider a single UAV that houses 5G SNPN equipment needed to form basic radio access for the UE-UAV$_{\text{gNB}}$-UE communications.

In rural and open-space areas, for the Line of Sight (LOS) scenarios, the Free Space Path Loss (FSPL) L_{FSPL} (in dB) can be estimated by applying the ITU-R P.525 model (within version 12 of ITU-R P.1411) that assumes minimal obstructions [24]. The LOS path loss equation is:

$$L_{FSPL} = 20log_{10}f + 20log_{10}d + 92.45 \quad (1)$$

In this equation, f is the frequency in GHz and d is the distance in kilometers between UAVgNB and UE.

In the feasibility study presented in this paper, Figure 2 depicts the principle of the UAV setup. For the baseline and comparative reference, this study is based on a theoretical omnidirectional UAV-mounted 0 dBi antenna. In practice, isotropic antenna gain is conservative whereas directive antenna enhances the link and optimizes the radio coverage also for minimizing the interference; an example of this is a cone-shaped vertical radiation pattern as depicted in Figure 3.

In field deployments, an adaptive Multiple-In Multiple Out (MIMO) antenna provides augmented performance, capacity, and interference mitigation, but the drawback is the increased complexity and power consumption. To keep the antenna complexity and respective power consumption at minimum in this study, passive omni-directional approach provides means to materialize multi-UAV gNB connectivity without a need for a specific steering logic.

In practice, for the final selection of the antenna type and respective gain, detailed radio network planning is important for ensuring adequate inter-UAV connectivity and radio cell dimensioning. The impact of the final antenna gain can be considered adjusting the presented G_{TX} parameter values.

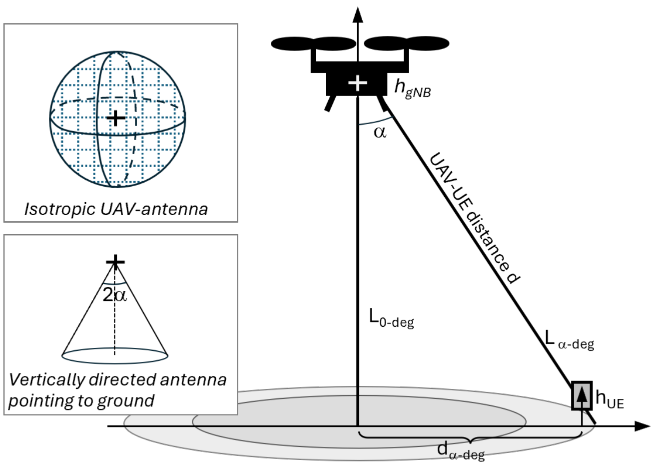

Figure 3. Principle of (theoretic) radiation patterns and respective radio coverage formation assumed in this study

VII. Results

Using ITU-R P.1411, Figure 4 presents the path loss UE-UAV at a distance *d* from UAV's location for isotropic UAV transmitter (TX) antenna at 100 m altitude (earth curvature limit 35 km) for frequency bands 1 GHz – 28 GHz.

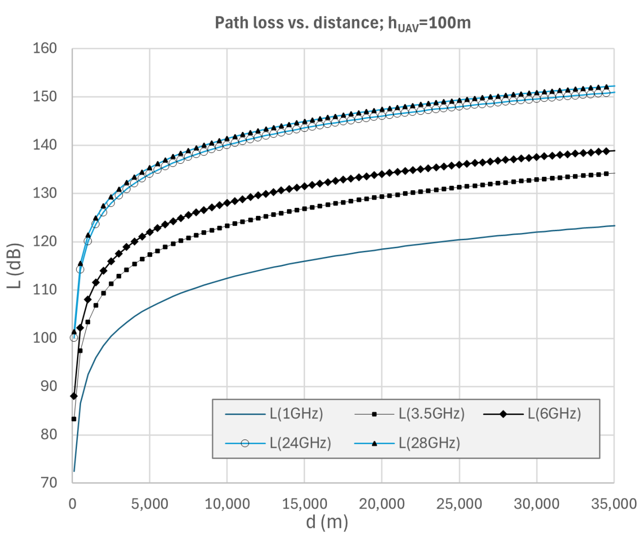

Figure 4. Path loss of UAV-UE as a function of the UE's distance from UAV's vertical reference location (UAV altitude is 100m)

Considering the same frequency range 1 GHz – 28 GHz, Figure 5 summarizes the estimated path loss values L (dB) directly beneath (α=0º) and off the vertical location of the UAV (α=30º) in open and rural areas, when the UAV altitude varies between 50 m and 400 m. The presented LOS path-loss estimates show that the altitude-distance trends for 1–28 GHz match the 3GPP TR 38.901 LOS baseline [25]. Comparable UAV-gNB studies at 28 GHz [26][13] show the same free-space path loss driven scaling, with practical shortfalls mainly from blockage, beam-pointing, and backhaul constraints rather than the LOS model itself. Consistent with geometry, off-nadir (30°) incurs about 1.25 dB extra loss from the longer slant range, and at 100 m altitude the footprint is curvature-limited. Deployment planning can thus start with FSPL-based bounds and subtract environment-specific losses for realistic coverage.

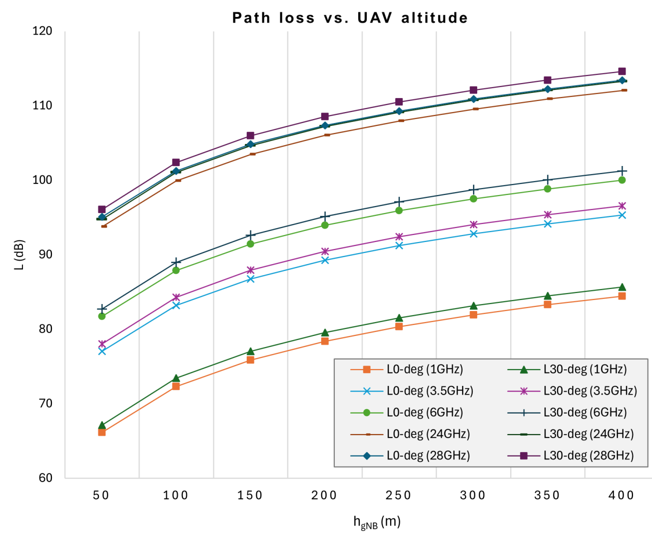

Figure 5. Path loss prediction, 1GHz–28GHz, for UAV altitudes of 50m–400m

A. Scenario: eMBB

Table V presents the key eMBB radio budget items, and Table VI presents an example of the radio link budget when the UAV altitude is 400 m and the UE is located underneath.

In these scenarios, the channel bandwidth is 20 MHz (1 GHz), 100 MHz (3.5/6 GHz), or 400 MHz (24/28 GHz). In these calculations, spectral efficiency model is η (bps/Hz) = $0.6\times\log_2(1+SNR)$. The assumption for the 0.6 factor is due to scheduler, modulator and coding inefficiencies that lower

TABLE V. Applied radio link budget items, eMBB scenario

Parameter	Value	Notes
gNB transmitter power P_{TX}	+23 dBm	Typical small-cell power limit, applicable to a UAV-mounted gNB
TX antenna gain G_{TX}	0 dBi	Isotropic (no beamforming)
UE antenna gain G_{RX}	0 dBi	Smartphone baseline
Fade margin M	3 dB	Covers body loss, ageing, fading
UE noise figure NF	7 dB	5G NR handset typical
Thermal noise density	–174 dBm/Hz	$N_o=kT=1.38\times10^{-23}$ J/K × 290K

TABLE VI. EXAMPLE OF THE RADIO LINK BUDGET (D=400M)

Link budget, h_{UAV}=400m, α=0°	**1 GHz**	**3.5 GHz**	**6 GHz**	**24 GHz**	**28 GHz**
Path loss PL, dB at (2km)	84.5	95.4	100.1	112.1	113.4
Tx power (gNB), dBm	23.0	23.0	23.0	23.0	23.0
Tx antenna gain, dB	0.0	0.0	0.0	0.0	0.0
UE antenna gain, dBi	0.0	0.0	0.0	0.0	0.0
Implementation/fade margin, dB	3.0	3.0	3.0	3.0	3.0
UE noise figure NF, dB	7.0	7.0	7.0	7.0	7.0
Thermal noise density, dBm/Hz	-174	-174	-174	-174	-174
Channel bandwidth, MHz	20	100	100	400	400
Received power Prx, dBm	-61.5	-72.4	-77.1	-89.1	-90.4
Noise floor N, dB	-94.0	-87.0	-87.0	-81.0	-81.0
Operational SNR after margin, dB	29.5	11.6	6.9	-11.1	-12.5
Spectral efficiency SE	5.88	2.38	1.54	0.06	0.05
Data rate, Mb/s	**117.6**	**237.5**	**154.4**	**25.8**	**19.1**

the theoretic capacity of Shannon limit. The received power is $P_{RX} = P_{TX} + G_{TX} + G_{RX} - L$, and the noise floor is N = -174 + 10 $\log_{10}B + NF$. The operational signal to noise ratio (SNR) after margin is SNR = $P_{RX} - N - M$. The spectral efficiency $SE = 0.6\times\log_2(1+10^{SNR/10})$, and the data rate is $R = SE \times B$. Beyond the presented calculations, the effective SINR enhances through beamforming gain G_{BF} that is typically 3-10 dB whilst the level of interference lowers it respectively. MIMO, in turn, adds rank often 1-2 aloft scaling efficiency, and resource allocation gives a per-UE share 0.3-0.8. [27]

Figures 6 and 7 summarize the impact of h_{UAV} (50 m – 400 m) on the received single user data rate considering the space below the UAV and surrounding region. The results are based on analytical modeling of path loss prediction and a set of radio link budget attribute values (select examples presented in Table V and VI), varying the UAV altitude.

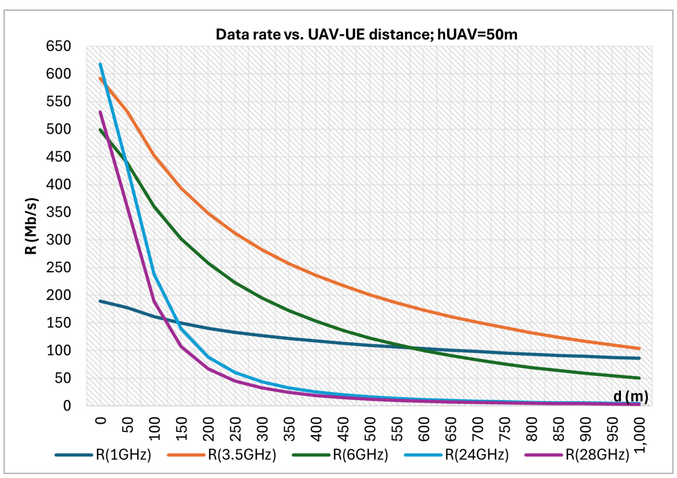

Figure 6. Data rate for UAV-mounted 5G gNB at 50 m altitude

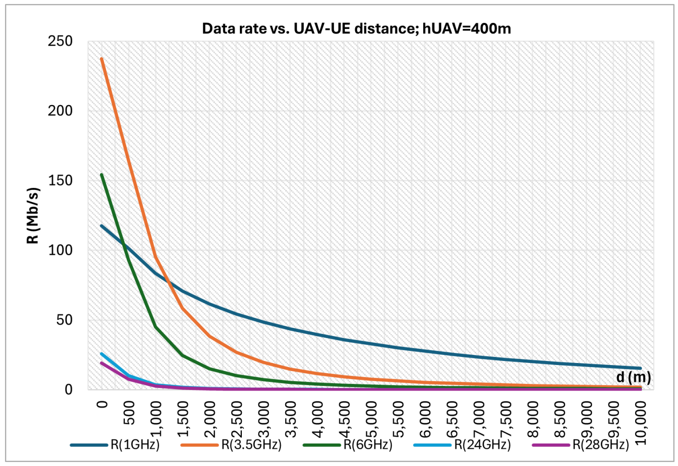

Figure 7. Data rate for UAV-mounted 5G gNB at 400 m altitude

As can be seen, high-band (24 GHz and 28 GHz) provides the highest rates when the distance between UAV_{gNB} and UE is relatively short, but the rate lowers drastically as the distance between UAV and UE increases over a few hundred meters due to the strong attenuation of this band. As can be expected, the mid-band (3.5 GHz and 6 GHz) performs more constantly at short distances and nearby regions.

Taking a closer look at the short distance (5–200 m) between the UAV and UE, Figure 8 shows more detailed behavior. As can be seen, high-band outperforms the other bands up to about 50 m distances providing 1–2 Gb/s data rates, but afterwards, mid-band provides the highest rate (250–500 Mb/s). The heavy attenuation of the high-band makes also the low-band data outperform it beyond 150–200 m distance.

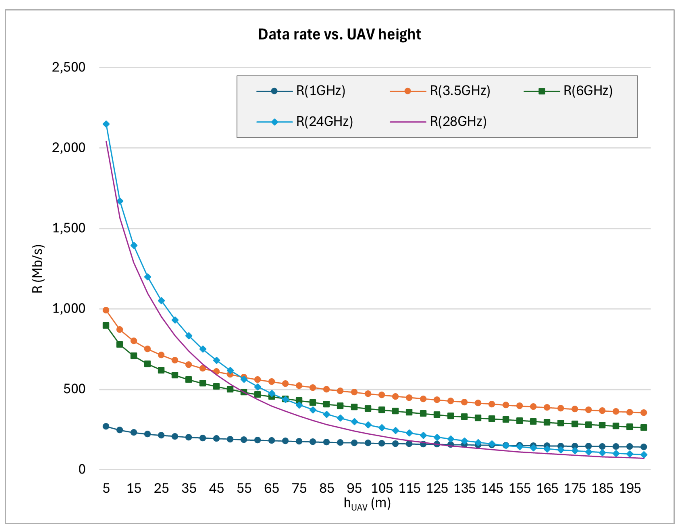

Figure 8. Data rate behavior when the distance between the UAV and UE is short (5-200m)

Figure 8 shows that for a critical mission in open and rural areas, assuming the key requirement is fast data connectivity and high capacity, e.g., for high-definition video contents, high-band provides optimal performance up to about 100 m.

If, instead, the main requirement is a large coverage area (e.g., over 10 km), and the UAV operation is possible at high altitude (e.g., 400 m), low-band is adequate selection as Figure 8 indicates. Should there be limitations for the UAV altitude, such as nearby airports or other restricted areas, mid-band (particularly 3.5 GHz) provides the most adequate balance for h_{UAV} and radio performance, as can be seen in Figure 6.

B. Scenario: IoT

Table VII presents key radio budget items for the IoT scenario comparing NB-IoT class CE0 and CE2, LTE-M, and RedCap.

TABLE VII. APPLIED RADIO LINK BUDGET ITEMS, IOT

Link budget	**NB-IoT$_{CE0}$**	**NB-IoT$_{CE2}$**	**LTE-M**	**Red Cap**
Channel bandwidth, MHz	0.18	0.18	1.40	5.00
Thermal noise floor, dBm	-114.4	-114.4	-105.5	-100.0
Impl. / fade margin, dB	8.0	14.0	8.0	5.0
Required SNR / E_b/N_o	-5.0	-13.0	-7.0	-3.0
RX sensitivity, dBm	-119.4	-127.4	-112.5	-103.0
Peak data rate, b/s	25k	50-100	1M	150M
Path loss budget, dB	**134.4**	**136.4**	**127.5**	**121.0**
Distance (1GHz), km	»35	»35	»35	2̃5
Distance (3.5GHz), km	3̃5	>35	1̃5	7̃

In all these cases, the gNB transmitter (TX) power is 23 dBm, TX and receiver (RX) antenna gains are 0 dBi, and RX noise figure is 7 dB (typical low-cost IoT modem). Again, the free-space path loss model is used in these calculations. Receiver sensitivity is driven by bandwidth, i.e., noise floor plus the required SNR for the lowest modulation / coding of each profile. Path-loss budget is the maximum loss the link can tolerate after allocating the fade / implementation margin. Converting that budget to free-space distance shows the theoretical cell radius; real-world coverage will be smaller due to UAV altitude (earth curvature), foliage, buildings and interference. The presented SNR / (E_b/N_0) values are for the lowest-order modulation / coding in each profile (reference sensitivity) as per the UE RF specifications [28][29], and the RX sensitivity is N + Required SNR (cross-checked with the specifications for minimum guaranteed UE sensitivity).

As can be seen, NB-IoT can reach the radio horizon even with only 23 dBm EIRP; coverage is limited by geometry, not RF. LTE-M at 1 GHz still covers tens of kilometers, whereas at 3.5 GHz it shrinks to about 15 km LOS. NR RedCap offers the highest data rates but requires roughly 10 dB more SNR than NB-IoT, confining its cell to single-digit-kilometer radii at 3.5 GHz. These Tables can be used directly to size UAV altitude, antenna gain, or additional power needed for a given IoT service profile. Compared with the broadband case (with MCL 95–105 dB), IoT enjoys tens of dB link budget head-room mainly from the narrow bandwidth and low SNR requirement. Thus, all the presented IoT cases outperform the radio coverage of the eMBB.

VIII. SIMULATIONS

As a step beyond conventional radio link budget estimates, our research team developed a simulation environment based on in-house software tools. The software was developed by the authors for use in normal terrain-based radio prediction modeling across 300-4,500 MHz Frequency Range 1 (FR1) bands and other modules for Frequency Range 2 (FR2) millimeter-wave systems, and has been modified to enable the generation of radio predictions from both static and mobile aerial base-station platforms.

The objective of these simulations was to evaluate practical deployment scenarios for a UAV-mounted 5G gNB and its associated antenna system. The simulation framework extends the default base-station configuration parameters used in typical terrestrial radio network planning tools, enabling the modeling of aerial radio nodes and their interactions with ground-based UEs.

The radio prediction modeling toolset is colloquially known as AARON. It is designed primarily to operate on servers with significant Graphics Processing Unit (GPU) capability, as it utilizes novel ray-tracing algorithms to develop the prediction layers, in conjunction with digital elevation models for the elevation data, with a resolution down to one square foot (0.093 m^2) per pixel, and supporting multiple different coordinate reference sets which may be used to ensure accurate alignment of terrain data and mapping representations.

The toolset allows for computation of Reference Signal Received Power (RSRP), Signal-to-Interference-plus-Noise Ratio (SINR), and cell capacity estimations, assuming fully utilized Resource Block (RB) allocations with consideration of the defined cells in the cell configuration file. This is available across the current approved range of Frequency Division Duplex (FDD) and Time Division Duplex (TDD) cellular frequencies, with differing bandwidths, from 1.4 MHz up to 100 MHz, and can be tailored for additional bandwidths, as required.

The AARON toolset contains a range of modules, including dedicated modules to extract and process elevation data from high-definition Light Detection and Ranging (LiDAR) data files (.LAZ format), which are typically available for many countries through central mapping agencies or data repositories.

The toolset can be configured for a range of computational parameters, particularly related to different antenna designs, where antenna beam roll-off, -3 dB vertical and horizontal beam width can be defined. There is support for massive MIMO antenna structures, with variable beam-counts, allowing for a User to define a specific antenna for a use case.

AARON supports different propagation models, with the use of free space loss as the default for the purposes described herein, with a modified COST-231 model is utilized for predictions using terrain-based base stations.

The toolset is configured through three Comma Separated Variable (.CSV) files, generated using an external text editor tool, providing the following files:

- Master File (for multiple project listings).
- Project Configuration file, where the defined project paths and tool configuration data is stored.

- Cell configuration file, which provides individual cell parameters, such as site location, antenna height, -3dB beamwidths, mechanical and electrical tilt parameters, RF power (typically RS power for LTE, and PBCCH block power for 5G).

This allows for relatively straight-forward adaptations and modification of the tool's behavior, for different prediction scenarios.

The toolset has some newly developed techniques for allowing a set of sequential predictions to be generated to emulate one or more mobile aerial base stations, as well as fixed ground stations to be defined. This allows for generating predictions for given time sequences and paths, and displayed as animated graphical presentation for the users.

In conventional radio network coverage prediction tools, the underlying assumptions typically reflect a tower-mounted base station antenna configuration. These models incorporate standard link-budget components such as feeder cable losses, connector attenuation, sector antenna orientation, and mechanical or electrical downtilt optimized for terrestrial coverage scenarios. However, in the case of a UAV-mounted gNB, several of these assumptions change due to the three-dimensional mobility of the aerial platform and the absence of fixed infrastructure.

For aerial base stations, antenna orientation and coverage patterns differ significantly from traditional sectorized cellular deployments. Rather than directing the antenna main lobe horizontally or slightly downward toward a predefined service area (such as a roadway corridor or urban sector) a UAV platform typically operates in a dynamic 3D environment. In such conditions, the antenna must provide coverage not only to ground users but potentially also to other aerial nodes, including additional UAV-mounted gNBs or UAV-based user equipment. This is especially relevant in rapidly deployable temporal aerial networks for fast response and disaster recovery [30]. Consequently, a practical and lightweight solution is the use of a passive omnidirectional antenna mounted on the UAV platform, enabling approximately uniform radio coverage in the surrounding airspace and toward the ground users beneath the drone.

In the simplest implementation, a passive omnidirectional antenna configuration can be approximated using a half-wave or full-wavelength dipole antenna. Such antennas offer relatively uniform azimuth radiation without requiring power-consuming beamforming hardware. This is advantageous for UAV platforms where payload weight and onboard energy consumption are critical constraints. Passive antennas require no additional signal processing or electronic beam steering, which reduces system complexity, weight, and power consumption compared to active antenna arrays or MIMO beamforming systems.

Figure 9 illustrates the well-known conceptual principle of an omnidirectional UAV antenna radiation pattern. This type of antenna can serve both ground users and aerial nodes within the surrounding three-dimensional space.

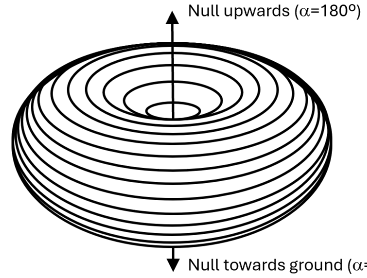

Figure 9. Principle of (close to) omnidirectional UAV antenna serving users on the ground and other UAV nodes in 3D space

To implement a simple, practical, and passive antenna element in the simulation environment, a 1-λ dipole antenna model was used. From a system engineering perspective, passive antennas provide several advantages for UAV-mounted gNB platforms. Active beamforming antennas, although capable of higher gain and adaptive beam steering, require additional RF chains, digital processing, and power amplifiers, which significantly increase both system mass and power consumption. For small and medium UAV platforms, the available payload capacity and onboard energy budget are limited. Therefore, passive antenna solutions often represent a realistic trade-off between performance, weight, complexity, and flight endurance. Several studies on UAV-based communication platforms emphasize that the communication payload, including the base station and antenna subsystem, must remain lightweight and energy-efficient in order to maintain practical flight durations and operational feasibility [30][31].

The radiation pattern of a dipole antenna is commonly described as "donut-shaped," where the maximum radiation occurs in directions perpendicular to the antenna axis, while nulls appear along the antenna axis itself. In the context of a UAV-mounted antenna, this means that the strongest radiation occurs horizontally around the UAV, while weaker radiation exists directly above and below the antenna.

At first glance, this radiation pattern might appear sub-optimal for ground coverage because the antenna exhibits a null directly beneath the UAV. However, in practical scenarios this limitation is partially mitigated by relatively short propagation distance between the UAV and ground-based user equipment directly below it, compared to the respective cell edge. The resulting free-space path loss reduction can compensate for the reduced antenna gain in the vertical direction.

To evaluate this effect, the first simulation rounds were conducted for the 3.5 GHz mid-band spectrum, which represents a common 5G deployment band worldwide. The simulated scenario considered a UAV-mounted gNB positioned above the Bondi Junction shopping center area in Sydney, Australia. The UAV altitude in this scenario was modeled to be approximately 500 m above ground level, which illustrates the capability for wide-area coverage for activities for search and rescue, or emergency service deployment in disaster zones. Please note that while regulation limits the maximum altitude of drones, in this specific case, the aim was to understand technical limitations applicable to these special use cases assuming the respective policies may be relaxed.

The initial prediction uses a singular static UAV, with a further prediction introducing an additional two static UAV's (one to the east, the second further south of the initial UAV), to simulate the impacts of interference on predicted downlink throughput. The radio parameters used in this simulation included a 100 MHz channel bandwidth, numerology μ = 1 (corresponding to 30 kHz sub-carrier spacing), and a total transmit power of 5 watts, consistent with currently approved RF power limitations for mid-powered cell equipment, and considered suitable for UAV payload integration. The antenna gain of the simulated dipole was 2.3 dBi in the main radiation directions.

Terrain data used in the simulation had a spatial resolution of approximately one meter, derived from LiDAR point-cloud measurements. Such high-resolution terrain information allows accurate modeling of ground elevation and environmental features affecting signal propagation. As illustrated in Figure 10, the relatively flat terrain in the Bondi Beach direction results in higher received signal strength compared with other directions at similar distances from the UAV. However, the coverage area directly beneath the UAV shows minimal reduction due to the "donut" effect due to the dipole antenna radiation null.

The signal pattern in Figure 10 suggests a relatively even spread of RF Power on the Downlink direction, minimizing "hot-spots" where UE Receiver may experience saturation levels, with signal distortion. When the additional UAV's are included in the prediction, the coverage prediction of Figure 11 shows widespread coverage across the majority of the area, with a central left-to-right band of marginally lower signal, from the lateral separation of UAV's 1 and 3.

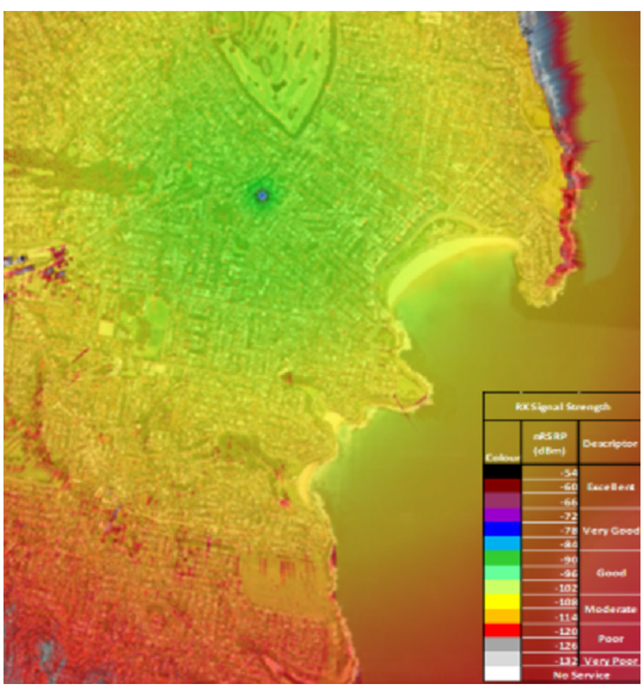

Figure 10. Singular Coverage prediction for UAV-mounted 5G gNB at 500 meters over Sydney area

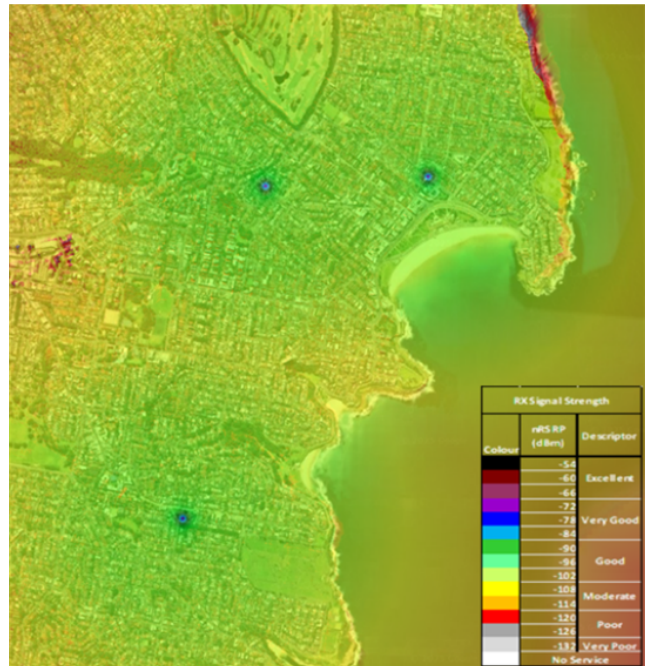

Figure 11. Three-UAV Coverage prediction for UAV-mounted 5G gNB at 500 m over Sydney area

The 5G-SA capacity prediction in Figure 12 illustrates the shortcomings of utilizing small separation between UAV's at a significant operating height, such as in this case, 500 meters.

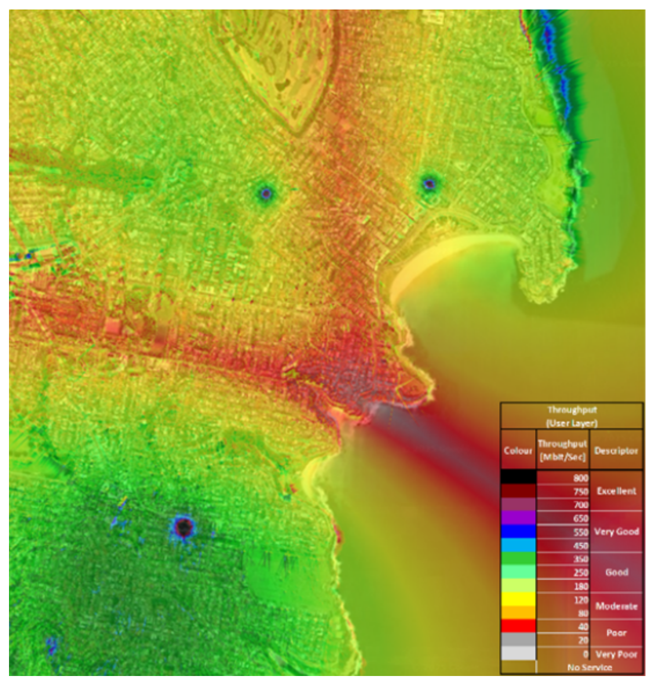

Figure 12. Three-UAV Capacity prediction for UAV-mounted 5G gNB at 500 m over Sydney area

There is significant reduction in the capacity capability of UAVs 1 and 2, due to the excessive overlap of the coverage between the two patterns, with a relatively broad swathe of low-capacity area running North-South as marked in the orange and red colors. A similar pattern is observed at the cell edges between UAV's 1 and 3, however it presents a a sharper delineation of red color, with narrower bands of orange.

This indicates the reduction of inter-cell interference at the cell edges, with a higher propensity for a clean "break" on the handover between the two (reduced cell "ping-ponging"). The additional lateral separation of UAV 3 can also be observed by the much larger area with dark-green, blue, and purple coloring, indicating significantly higher downlink throughput capability compared to that of UAV 1 and UAV 2, which are in proximity.

The second simulation round was conducted for UAV's at an altitude of 200 m. In this case, the antenna gain was assumed to be approximately 6.5 dBi, representing a slightly higher-gain omnidirectional antenna configuration. The effective transmit power was approximately 2 W total cell power, corresponding to small-cell-class gNB equipment designed for portable or aerial deployments.

Compared to the first scenario, the higher altitude increases the overall coverage radius of the UAV cell, although at the expense of reduced received signal strength at longer distances due to increased free-space path loss. This reflects the typical trade-off between coverage area and signal quality when determining the optimal UAV operating altitude.

Figure 13 illustrates the resulting signal strength distribution at the same geographical location. For the selected parameter values, i.e., 100 MHz bandwidth, numerology $\mu = 1$ (30 kHz subcarrier spacing), and approximately 2 W total cell transmit power, the simulated data rate distribution is consistent with expectations for a lightweight aerial small-cell system operating in the 3.5 GHz band.

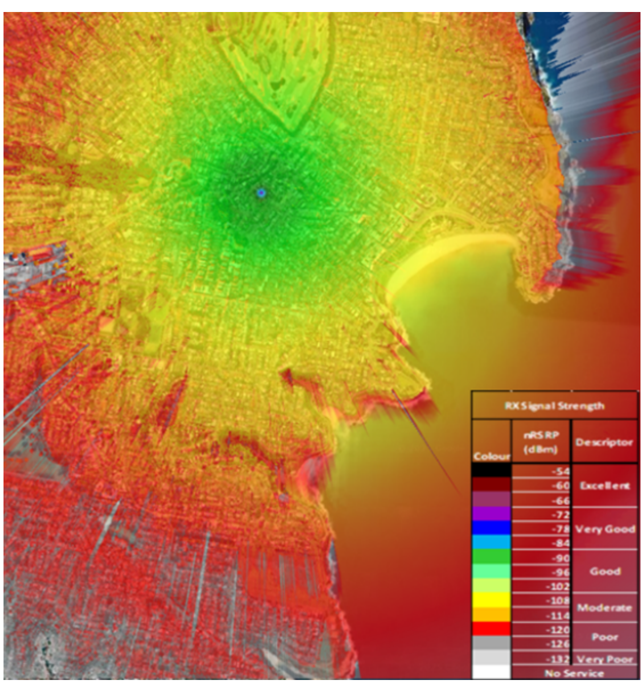

Figure 13. Singular Coverage for UAV-mounted 5G gNB over Sydney area at 200 m altitude

Figures 14 and 15 illustrate how lower altitude, combined with lower transmit power and higher-gain antennae assist in providing a tighter coverage performance, with significant improvements in cell-delineation, greater areas with high capacity coverage, and increases in all UAV zones of areas where high Downlink Throughput can be expected.

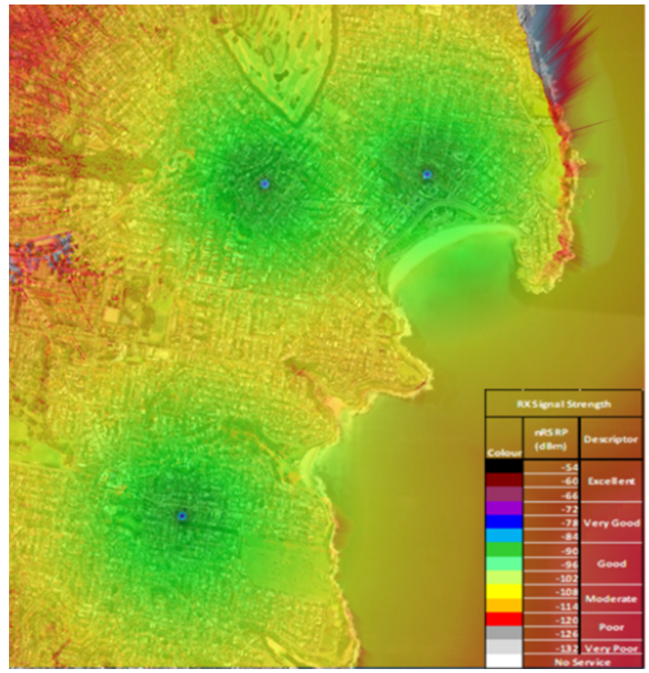

Figure 14. Three-UAV Coverage prediction for UAV-mounted 5G gNB at 200 m over Sydney area

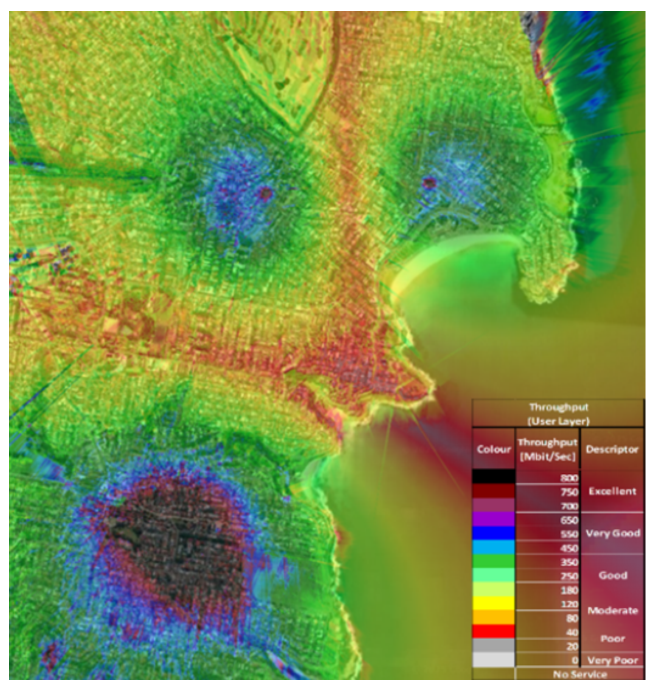

Figure 15. Three-UAV Capacity prediction for UAV-mounted 5G gNB at 200 m over Sydney area

Comparing the two scenarios highlights several important observations. At lower altitudes, the UAV provides stronger signal levels and higher data rates within a tighter coverage footprint. At higher altitudes, the coverage area expands significantly, but the average throughput per user decreases due to increased path loss. These results are consistent with findings reported in several UAV-base-station studies, which indicate that there exists optimal UAV altitudes and spatial separation that balances coverage radius and signal quality depending on the deployment environment and service requirements.

IX. Summary

This study demonstrates that a single-UAV 5G SNPN assembled from COTS components can provide rapid, standards-based connectivity for both eMBB and IoT use cases, particularly in open or rural terrain environments.

Using the ITU-R P.1411 LOS propagation formulation as the baseline model, we analyzed how operating frequency (1–28 GHz) and UAV altitude (50–400 m) influence the trade-off between coverage area and achievable throughput. The observed altitude–distance relationships and off-nadir propagation characteristics are primarily driven by FSPL. At lower altitudes, coverage is limited primarily by geometric footprint constraints, while at higher altitudes the achievable range becomes increasingly dominated by path loss.

Millimeter-wave bands offer the highest short-range data rates but degrade rapidly with increasing distance due to higher path loss and sensitivity to blockage. In contrast, mid-band frequencies such as 3.5–6 GHz provide a balanced compromise between coverage radius and throughput, making them particularly suitable for UAV-mounted cellular nodes. Lower frequencies near 1 GHz can maximize coverage area at higher altitudes but offer reduced overall system capacity.

Link-budget templates developed for eMBB and IoT traffic profiles further show that IoT connectivity typically benefits from much larger link margins due to narrower bandwidths and lower signal-to-noise ratio requirements. In many IoT scenarios, the coverage limit is determined more by geometric line-of-sight constraints than by radio link budget limitations.

From a practical deployment perspective, the simulations confirm that many principles used in conventional radio network planning tools can be adapted for UAV-mounted gNB systems. However, several additional considerations must be incorporated when modeling aerial cellular nodes related to adequate antenna selection, understanding power and payload constraints, impact of altitude, differences in 3D modeling in terms of mobility and positioning.

Lightweight passive omnidirectional antennas are often preferred for UAV platforms due to their low power consumption and reduced system complexity. Active beamforming arrays can provide higher gain but significantly increase energy consumption and payload weight, so the passive antenna approach may be critical in the lowest power consumption scenarios. Of the power and payload constraints in general, the onboard power budget and payload capacity of the UAV impose strict limits on radio hardware selection and transmission power levels. This study shows that optimal altitude selection is one of the key tasks as UAV altitude must balance coverage area, path loss, regulatory restrictions, and flight endurance.

For the 3D coverage aspects, unlike is the case in terrestrial networks, aerial base stations require modeling of coverage both horizontally and vertically to account for ground users and aerial nodes so that UAV movement can be exploited to dynamically optimize coverage, capacity, and interference conditions. Modeling of interference interactions between dynamic SNPN gNBs and co-channel terrestrial gNBs need to be explored, too, in detailed 3D radio network planning.

This presented experimentation shows significant promise toward developing clear guidelines for complex environments where intelligent decision-making for gNB positioning, flight-paths and use of terrain features are critical for real-time interference management. These results provide useful baseline parameters for future studies involving multi-UAV aerial networks, cooperative UAV base station deployments, and AI-assisted network optimization.

X. Future Research

Building upon the presented research, our future work will expand the evaluation of UAV-mounted 5G networks across a broader range of terrain environments, including low-rise suburban areas and dense urban environments with high-rise buildings with respective radio propagation models capable of capturing complex air-to-ground channel characteristics. Our further research will also aim to explore multi-UAV network architectures where multiple drone-mounted gNBs operate collaboratively to form aerial cellular networks. Such systems may employ wireless backhaul links between UAVs or IAB architectures to extend network coverage dynamically and algorithms to optimize the inter-UAV distances as a function of the UAV altitude, considering the balancing of provided coverage and capacity. These characteristics will support a range of more complex use cases particularly directed toward geo-location capabilities for search and rescue and similar activities.

Another important, potential research direction involves the use of artificial intelligence and machine learning methods for UAV network coordination. AI-assisted positioning algorithms could enable autonomous UAV placement based on real-time user distribution, traffic demand, and interference conditions. Recent research suggests that intelligent UAV placement and trajectory optimization can significantly improve network performance, coverage fairness, and energy efficiency in aerial communication systems.

Finally, advanced sensing technologies and environmental awareness may allow UAV-mounted gNB systems to dynamically adapt their position, altitude, and transmission parameters in response to changing radio conditions, interference patterns, and user mobility. Such capabilities, derived from, e.g., 3GPP's ISAC (Integrated Sensing and Communication) work item could enable fully autonomous aerial communication networks capable of rapid deployment during emergency situations, temporary events, or infrastructure outages.

ABBREVIATIONS

3GPP 3rd Generation Partnership Project
5G Fifth Generation mobile communications
6G Sixth Generation mobile communications
AGL Above Ground Level
B5G Beyond 5G
CN Core Network
COTS Commercial Off-the-Shelf
CoW Cell on Wings
CSV Comma Separated Variable
EASA European Union Aviation Safety Agency
EIRP Effective Isotropic Radiated Power
eMBB evolved Mobile Broadband
FDD Frequency Division Duplex
FSPL Free Space Path Loss
gNB Next Generation Node B
GPU Graphics Processing Unit
GSMA GSM Association
HARQ Hybrid Automatic Repeat Request
IAB Integrated Access and Backhaul
IoT Internet of Things
ISAC Integrated Sensing and Communication
LiDAR Light Detection and Ranging
LiPo Lithium Polymer
LOS Line of Sight
LTE Long-Term Evolution
LTE-M LTE for Machines
MIMO Multiple-In Multiple Out
mMTC Massive Machine Type Communications
MNO Mobile Network Operator
NB-IoT Narrow-Band IoT
NF Network Function
NFV Network Functions Virtualization
NPN Non-Public Network
NR New Radio
NS Network Slice
NSI Network Slice Instance
NSP Network Slice Provider
NTN Non-Terrestrial Network
PBCCH Physical Broadcast Channel
PLMN Public Land Mobile Network
PNI Public Network Integrated
QoS Quality of Service
RAN Radio Access Network
RB Resource Block
RedCap Reduced Capabilities
RF Radio Frequency
RS Reference Signal
RSRP Reference Signal Received Power
RX Receiver
SBA Service-Based Architecture
SBI Service-Based Interface
SINR Signal-to-Interference-plus-Noise Ratio
SNPN Standalone Non-Public Network
SNR Signal-to-Noise Ratio
TDD Time Division Duplex
TIP Telecom Infra Project
TX Transmitter
UAS Uncrewed Aerial Vehicle
UE User Equipment

ACKNOWLEDGEMENT

We gratefully acknowledge the feedback of Professors M. Reisslein, G. Trichopoulos, S. Zeinolabedinzadeh, and A. Alkhateeb of Arizona State University on the link budget considerations of this work.

REFERENCES

[1] J. Penttinen, "Design Feasibility and Link Budget Assessment of Aerial 5G IoT and eMBB Connectivity," The First International Conference on AI-enabled Unmanned Autonomous Vehicles and Internet of Things for Critical Services, IARIA AIVTS 25, Barcelona, Spain, pp 1-7, 2025.
[2] 3GPP, "TR 38.865: Study on further NR RedCap UE complexity reduction," 2022.
[3] GSMA, "Mobile economy report 2025," GSMA Intelligence, London, UK, 2025.
[4] J. Penttinen, "On 6G visions and requirements," Journal of ICT Standardization, vol. 9, no. 3, pp. 311-325, 2021.
[5] P. Jain, "3GPP SA 6G planning and progress," 3GPP, 2024.
[6] G. Wikstrom and S. Thorson, "Explore the impact of 6G," Ericsson, 19 December 2024. https://www.ericsson.com/en/blog/2024/12/explore-the-impact-of-6g-top-use-cases-you-need-to-know. Accessed 6 May 2026.
[7] O-RAN Alliance, "Who we are," https://www.o-ran.org/who-we-are. Accessed 6 May 2026.
[8] Telecom Infra Project (TIP), "How TIP Works," https://telecominfraproject.com/how-we-work/. Accessed 6 May 2026.
[9] Ericsson, "Industrializing Open RAN," https://www.ericsson.com/en/openness-innovation/open-ran-explained. Accessed 5 May 2026.
[10] M. Mushi, Y. Liu, S. Sreenivasa, O. Ozdemir, I. Guvenc et al., "Open RAN testbeds with controlled air mobility," Computer Communications, vol. 228, Article 107955, 2024.
[11] M. Saym, M. Mahbub, and F. Ahmed, "Coverage maximization by optimal positioning and transmission planning for UAV-assisted wireless communications," in International Conference on Science & Contemporary Technologies (ICSCT), Dhaka, Bangladesh, pp. 294-297, 2021.
[12] Y. Aydin, G. Karabulut, E. Ozdemir, and H. Yanikomeroglu, "Group handover for drone base stations," IEEE Internet of Things Journal, vol. 8, no. 18, pp. 13876-13887, 2021.
[13] M. Alamgir and B. Kelley, "Fixed Wing UAV-based Non-Terrestrial Networks for 5G millimeter wave Connected Vehicles," in IEEE 13th Annual Computing and Communication Workshop and Conference (CCWC), pp. 1167-1173, 2023.
[14] A. Fouda, A. Ibrahim, and I. Guvenc, "UAV-Based in-band Integrated Access and Backhaul," in IEEE 88th Vehicular Technology Conference (VTC-Fall), Chicago, IL, USA, pp. 1-5, 2018.
[15] S. Howe, "ATT's flying COW transmits 5G network by tethered drone," Commercial UAV News, 29 June 2022. https://www.commercialuavnews.com/public-safety/at-t-s-flying-cow-transmits-5g-network-by-tethered-drone. Accessed 6 May 2026.
[16] N. Tafintsev, A. Chiumento, O. Vikhrova, M. Valkama, and S. Andreev, "Utilization of UAVs as flying base stations in urban environments," in 15th International Congress on Ultra Modern Telecommunications and Control Systems and Workshops (ICUMT), Ghent, Belgium, pp. 7-11, 2023.
[17] P. Valente, A. Teixeira, M. Luis, D. Raposo, P. Rito, and S. Sargento, "Easy to deploy UAV-based non-public open-source 5G network," in 15th International Conference on Network of the Future (NoF 2024), Barcelona, Spain, pp. 72-80, 2024.
[18] J. Penttinen, J. Collin, and J. Pellikka, "On Techno-Economic Optimization of Non-Public Networks for Industrial 5G Applications," in The Nineteenth Advanced International Conference on Telecommunications (AICT 2023), Nice, France, pp. 1-7, 2023.
[19] 3GPP, "TS 23.501: System architecture for the 5G System (5GS)," 2025.

[20] 3GPP, "TS 23.548: 5G System Enhancements for Edge Computing; Stage 2," 2025.
[21] 3GPP, "TS 22.261: Service requirements for the 5G system," 2025.
[22] DJI, "Support for Matrice 300 RTK," https://www.dji.com/support/product/matrice-300. Accessed 6 May 2026.
[23] "Drone power feed through ground tethering," 17 April 2025. https://yle.fi/a/74-20156841. Accessed 6 May 2026.
[24] ITU, "Recommendation P.1411-12 (08/2023)," ITU-R, August 2023. https://www.itu.int/rec/R-REC-P.1411-12-202308-I/en. Accessed 6 May 2026.
[25] 3GPP, "TR 38.901: Study on channel model for frequencies from 0.5 to 100 GHz (Release 19)," 2025.
[26] M. Gapeyenko, I. Bor-Yaliniz, S. Andreev, H. Yanikomeroglu, and Y. Koucheryavy, "Effects of Blockage in Deploying mmWave Drone Base Stations for 5G Networks and Beyond," in IEEE International Conference on Communications Workshops, ICC, Kansas City, MO, USA, pp. 1-6, 2018.
[27] 3GPP, "TS 38.214 (V19.0): NR physical layer procedures for data (Release 19)," 2025.
[28] 3GPP, "TS 36.141: E-UTRA; Base Station conformance testing," 2025.
[29] 3GPP, "TS 36.101: E-UTRA; User Equipment radio transmission and reception," 2025.
[30] Y. Worku,C. Christodoulou, and M. Devetsikiotis, "UAV-Mounted Base Station Coverage and Trajectory Optimization Using LSTM-A2C with Attention," in Drones 2025, 9(11), 787, pp. 1-25.
[31] A. Abubakar, M. Mollel, O. Onireti, M. Ozturk, I. Ahmad et al. "Coverage and throughput analysis of an energy efficient UAV base station positioning scheme," Computer Networks, Vol 232, August 2023, 109854.